https://doi.org.10.3126/batuk.v9i2.57032
THE BATUK : A Peer Reviewed Journal of Interdisciplinary Studies
Vol. 9, Issue No. 2, July 2023, Page: 51-62
ISSN 2392-4802 eISSN 2565-4934
Received: 10 May 2023 Revised: 24 July 2023 Accepted: 27 July 2023

Prediction of Direct and Diffuse Solar Radiation on Pokhara, Nepal

*Prakash M. Shrestha[1,2], Narayan P. Chapagain[3], Indra B. Karki[1], and Khem N. Poudyal[4]

Abstract

The measurement of direct and diffuse solar radiation is not easily possible because instruments are quite expensive. The main objective of this study was to predict direct solar radiation (I_B) and diffuse solar radiation (I_D) on Pokhara (28.186643^o N, 83.97518^o E, 800 m asl) for a period of one year (2017). Daily data of spectral Aerosol optical depth (AOD) and total ozone column are obtained from NASA website. The maximum value of direct solar radiation and diffuse solar radiation values were found 932.9 ± 65.9 W/m^2 in January and 363.0 ± 87.9 W/m^2 in February respectively. The minimum value of direct solar radiation and diffuse solar radiation values were found 692.8 ±142.0 W/m^2 in April and 107.7 ± 20.4 W/m^2 in July respectively. The diffuse solar radiation changes with season. The annual average of direct solar radiation and diffuse solar radiation are found 808.1± 133.7 W/m^2 and 220.8 ± 102.8 W/m^2 and respectively. The results of this research work will help further identification, impact and analysis of solar radiation in different locations in Nepal with the same geographic conditions.

Keywords: aerosol, atmospheric transmittance, diffuse, direct radiation, solar radiation

1. Introduction

Since the sun is the closest star to the earth, solar energy is our basic and primary source of energy. The Sun radiates 4x 10^{26} W energy in forms of electromagnetic wave of wavelength 0.3µm to 3 µm (Poudyal et al., 2012). As the orbit of the Earth around the Sun is elliptical, the solar radiation decreases as square of distance between the Sun to the Earth. 1367 W/m^2 (I_{sc}) solar energy incidents on the outer surface of Earth's atmosphere when distance between Sun and Earth is 1.49x10^8 km (Duffie & Beckman, 2013). The solar radiation (I_0) incidents on specific point of outer surface of atmosphere at specific time depends on day number of year (DOY, n_d) (Iqbal, 1983).

$$I_o = I_{sc}\left[1 + 0.033\cos\left(\frac{2\pi}{365}n_d\right)\right] \quad (1)$$

[1] Department of Physics, Patan Multiple Campus, IoST, T U
[2] Central Department of Physics (CDP), IoST, T U
[3] Department of Physics, Amrit Campus, IoST, TU
[4] Department of Physics,Pulchowk Engineering Campus, IoE ,T U
*Correspondence concerning this article should be addressed to Prakash M. Shrestha, Patan Multiple Campus, Pulchowk, Lalitpur. Email: prakash.shrestha@pmc.tu.edu.np

When solar radiation passes through the atmosphere, it interacts with constituents of the atmosphere. The solar radiation is scattered, reflected, and absorbed in the atmosphere. The solar radiation is attenuated in atmosphere. The solar radiation incident on the ground in two ways, direct and diffuse (Liou, 2002). The sum of those two solar radiations; direct solar radiation (I_B) and diffuse solar radiation (I_D) gives global solar radiation (GSR) (Bason, 2004).

Nepal is situated between latitudes of 26.36° N to 30.45° N and longitudes of 80.06° E to 88.2° E in South East Asia. The elevation of the country ranges from 60 m to 8848 m within a span of 200 km from south to north and about 800 km from east to west (Majupuria,1999). In developing countries like Nepal, the most of energy consumption is fuel wood, agriculture residue, cow dung, coal and petroleum product. There is only 2.4 % (MoF, 2022) of energy consumption is alternative energy line hydroelectricity and solar. Nepal is land lock between two giant industrial countries India and China and their industrial byproduct can directly affects concentration of atmospheric components above Nepal. Nepal has to facility of sun tracker pyrheliometer and diffuse pyranometer to measure direct solar radiation and diffuse solar radiation respectively. Therefore, estimation of direct and diffuse solar radiation is necessary. Its application is very important on agriculture, Hydrology, Climate change, and energy harvesting (Poudyal et al., 2013).

Pokhara (28.186643° N, 83.97518° E, 800 m asl) lies in Kaski district of Gandaki Province as shown in Figure 1. Pokhara is capital of Gandaki Province and headquarter of Kaski district. Pokhara is the city of lakes (like Phewa, Begnas, Rupa). Three peaks Dhaulagiri, Annapurna, Manaslu with more than 8000 m height can be seen from the city. The Machhapuchchhre (Fishtail) with height of 6,993 metres is the closest to the city. Pokhara covers 464.24 square km. Pokhara has population 599,504 and population density 1,300 per square km (CBS, 2023). Average temperatures is between 25 and 35° C in summer and is -2 to 15° C in winter. Pokhara areas receive a high amount of precipitation in the country. Pokhara and nearby areas receive a high amount of precipitation 3,350 mm/year. Yearly mean daily GSR is 16.499 MJ/m^2/day from 2007 to 2012 in Pokhara (Adhikari et al., 2013). Maximum GSR is 23.21 MJ/m^2/day in June and minimum is 12.04 MJ/m^2/day in December from 2009 to 2010 in Pokhara (Poudyal, 2015).

Figure 1

Map of Pokhara

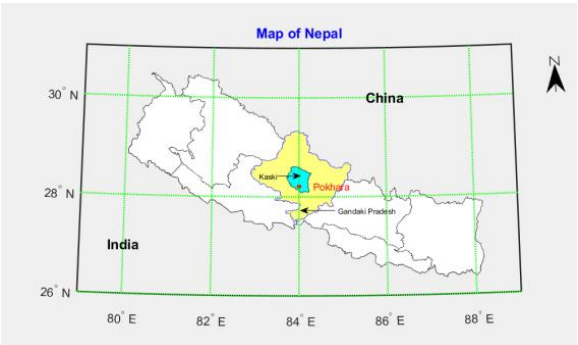

Note. The map is sourced from the website of Survey Department, Government of Nepal

2. Methods

The solar radiation is scattered, reflected, and absorbed by the atmospheric constituents like gas molecules, aerosols, water vapor, ozone and clouds. The solar radiation is attenuated in atmosphere with extinction coefficient (k) and optical air mass (m) (Lothian, 1963). The solar radiation incident on ground is two ways, direct and diffused.

Bird and Hulstrom (1981) developed Parameterization Model C for direct solar radiation (I_B) and diffuse solar radiation (I_D). Direct solar radiation (I_B)

$$I_B = I_o(0.9751\ \tau_o\ \tau_w\ \tau_g\ \tau_a\ \tau_r + B(z) \quad (2)$$

Here τ_o is atmospheric transmittance due to ozone, τ_w is atmospheric transmittance due to water vapor, τ_g is atmospheric transmittance due to gas mixture, τ_a is atmospheric transmittance due to aerosol and τ_r is atmospheric transmittance due to Rayleigh scattering. τ_o depends on ozone column (l) and relative air mass (m_r). τw depends on water content (w) and relative air mass. τ_g and τ_r depend absolute air mass (m_a). τ_a depends on Angstrom turbidity coefficient (β), Angstrom exponential (α) and absolute air mass (Wang et al., 2017). B(z) is a correction term for altitude (z) in meter (Bintanja,1996).

$$\tau_o = 1 - [0.1611\ u_3(1 + 139.48\ u_3)^{-0.3035}\ 0.002715\ u_3(1 + 0.044\ u_3 + 0.0003\ u_3^2)^{-1}$$

$$\tau_w = 1 - 2.4959\ u_1[(1 + 79.034\ u_1)^{0.682} + 6.385\ u_1]^{-1}$$

$$\tau_g = e^{[-0.0127 m_a^{0.26}]}$$

$$\tau_a = (0.1244\ \alpha\ -\ 0.0162)\ +\ (1.003\ -\ 0.125\ \alpha)e^{[-\beta\ m_a(1.089\ \alpha + 0.5123)]}$$

$$\tau_r = e^{[-0.0903\ m_a^{0.83}(1.01\ +\ m_a\ -\ m_a^{1.01})]}$$

Where

$$u_3 = l\ m_r$$

$$u_1 = w\ m_r$$

Diffuse solar radiation (I_D) is

$$I_D = I_{dr} + I_{da} + I_{dm} \quad (3)$$

where I_{dr} is diffuse solar radiation produced by Rayleigh scattering, I_{da} is diffuse solar radiation produced by aerosols and I_{dm} is diffuse solar radiation produced by multiple reflections.

$$I_{dr} = 0.79 I_0 cos\theta_z\ \tau_o\ \tau_g\ \tau_w\ \tau_{aa}\ \frac{0.5(1-\tau_r)}{1-m_a+m_a^{1.02}} \quad (4)$$

Here τ_{aa} is the atmospheric transmittance of aerosol absorptance. θz is solar zenith angle.

$$I_{dm} = \frac{(I_B cos\theta_z + I_{dr} + I_{da})\ \alpha_g\ \alpha_a}{1-\alpha_g\ \alpha_a} \quad (5)$$

α_g and α_a are albedo of ground and atmospheric albedo respectively.

$$I_{da} = 0.79 I_0 cos\theta_z\ \tau_o\ \tau_g\ \tau_w\ \tau_{aa}\ F_c \frac{0.5(1-\tau_{as})}{1-m_a+m_a^{1.02}} \quad (6)$$

Here τ_{as} is the atmospheric transmittance of aerosol scattering and $F_c = 0.84$.

Open source software Python 3.7 software is used to analysis data and to plot graph. Mean ($\bar{x}$), standard deviation (σ) are used as Statistical tool. Standard error (SE) is used as error bar in graph. Data is presented in form of '$\bar{x} \pm \sigma$'. Quartile (Q_1, Q_2, Q_3), skewness (γ_1) and (γ_2) are used to investigate nature of distribution of data.

$$SE = \frac{\sigma}{\sqrt{n}} \quad (7)$$

Here, n is number of data

$$\gamma_1 = \sqrt{\frac{\mu_3^2}{\mu_2^3}} \quad (8)$$

$$\gamma_2 = \frac{\mu_4}{\mu_2^2} - 3 \quad (9)$$

where μ_2, μ_3, μ_4 are 2nd, 3rd and 4th moment respectively.

Correlation coefficient (r) is used to find relation between two variable x and y.

3. Results

Daily ground base measurement of spectral aerosol optical depth (AOD) derive from AERONET of NASA and satellite measurement of Total ozone column (TOC) downloaded from NASA website for Pokhara for year 2017. Five wavelength (λ) 675, 500, 440, 380 and 340 nm are used to calculate Angstrom turbidity coefficient (β) and Angstrom exponential (α) by linear regression method for Angstrom model (Angstrom, 1961).

$$AOD = \beta\lambda^{-\alpha} \quad (10)$$

By using equation (1), (2), (3) and τ_o, τ_w, τ_g, τ_a, τ_r, daily direct radiation (I_B) and diffuse solar radiation (I_D) are calculated. Daily diffuse solar radiation produced by Rayleigh scattering (I_{dr}), diffuse solar radiation produced by aerosols (I_{da}) and diffuse solar radiation produced by multiple reflections (I_{dm}) are calculated by using equation (4), (5) and (6). Daily variation of I_{dr}, I_{dm} and I_{da} are shown in Figure 2. Figure 2(a) shows daily variation of diffuse solar radiation produced by Rayleigh scattering (I_{dr}). The maximum and minimum value of I_{dr} during study period of 2017 are found 38.8 W/m^2 and 30.1 W/m^2 respectively. The annual mean and standard deviation are found 34.8 W/m^2 and 2.4 W/m^2 respectively. Figure 2(b) shows daily variation of diffuse solar radiation produced by multiple reflections (I_{dm}). The maximum and minimum value of I_{dm} during the study period are found 65.1 W/m^2 and 11.0 W/m^2 respectively. The annual mean and standard deviation are found 37.9 W/m^2 and 10.3 W/m^2 respectively. Figure 2(c) shows daily variation of diffuse solar radiation produced by aerosols (I_{da}). The maximum and minimum value of I_{da} during the study period are found 480.3 W/m^2 and 24.5 W/m^2 respectively. The annual mean and standard deviation are found 480.0 W/m^2 and 92.5 W/m^2 respectively.

Figure 2(d) shows daily variation of diffuse solar radiation (I_D). The maximum and minimum value of I_D during the study period are found 580.4 W/m^2 on March 28 and 81.6 W/m^2 on July 22 respectively due to air pollution. The annual mean and standard deviation are found 220.8 W/m^2 and 102.8 W/m^2 respectively.

Figure 2

Daily Variation of Diffuse Solar Radiation

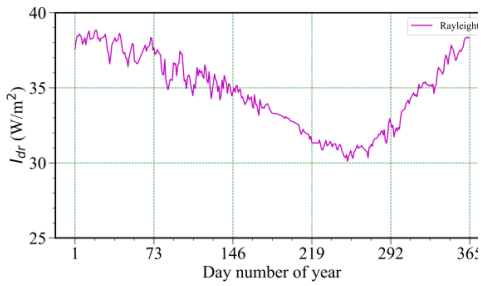

a) Daily variation of diffuse solar radiation due to Rayleigh scattering

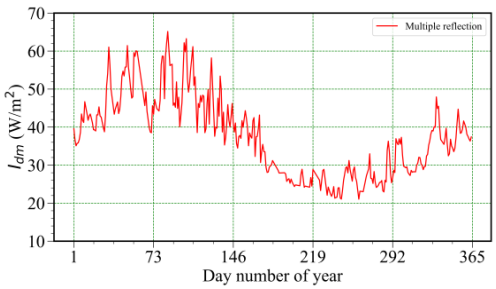

b) Daily variation of diffuse solar radiation due to Multiple reflection

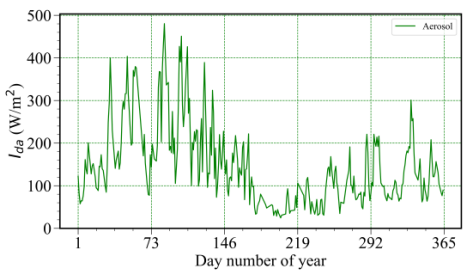

c) Daily variation of diffuse solar radiation due Aerosol

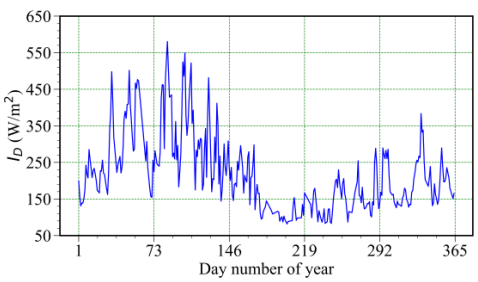

d) Daily variation of diffuse solar radiation

Figure 3(a) shows daily variation of direct solar radiation (I_B) and figure 4(a) shows corresponding histogram. The maximum and minimum value of I_B during study period of 2017 are found 1037.1 W/m^2 on January 3 and 354.2 W/m^2 on March 28 respectively. The annual mean and standard deviation are found 808.1 W/m^2 and 133.7 W/m^2 respectively. The first quartile (Q_1), second quartile (Q_2, median) and third quartile (Q_3) are found 736.3 W/m^2, 841.0 W/m^2 and 910.1 W/m^2 respectively. Skewness (γ_1) and kurtosis (γ_2) are found -0.89 and 0.33 respectively. The distribution of I_B is negatively tailed due to negative value of skewness and is not normal (Gaussian). For normal distribution, kurtosis must be zero. Out of 313 days of study period, 102 days has direct solar radiation between 800 W/m^2 to 900 W/m^2. Figure 3(b) shows ratio of diffuse solar

radiation (I_D) to direct solar radiation (I_B). Out of 313 days of study period, 7 days have I_D is greater than I_B. Those days are cloudy day.

Figure 3

Daily Variation of Direct Solar Radiation

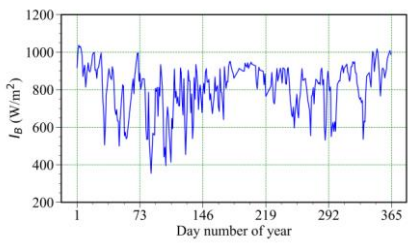

a) Daily variation of direct solar radiation

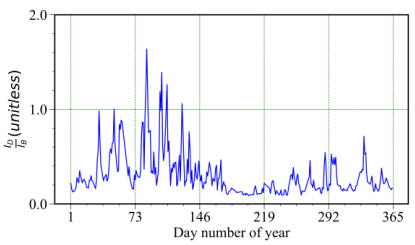

b) Ratio of diffuse solar radiation to direct solar radiation

Figure 4(b) shows histogram of diffuse radiation (I_D). The first quartile (Q_1), second quartile (Q_2, median) and third quartile (Q_3) of diffuse solar radiation are found 144.1 W/m^2, 199.3 W/m^2 and 266.2 W/m^2 respectively. Skewness (γ_1) and kurtosis (γ_2) are found 1.12 and 0.94 respectively. The distribution of I_D is positively tailed as skewness is positive and is not Gaussian (normal). Out of 313 days of study period, 134 days has direct solar radiation between 100 W/m^2 to 200 W/m^2.

Figure 4

Histogram of Direct Solar Radiation and Diffuse Solar Radiation

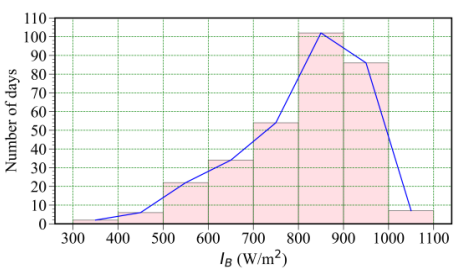

a) Histogram of direct solar radiation

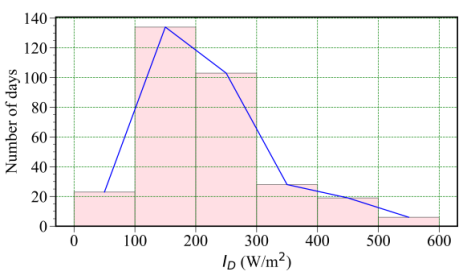

b) Histogram of diffuse solar radiation

Figure 5 shows monthly variation of direct solar radiation (I_B) and direct diffuse solar radiation (I_D). Figure 5(a) shows monthly variation of direct solar radiation (I_B). The maximum and minimum value of I_B during the study period are found 932.9 ± 65.9

W/m^2 in January and 692.8 ± 142.0 W/m^2 in April respectively. Variation is large in March due to large value of standard deviation 184.7 W/m^2 and less in July due less value in standard deviation 36.0 W/m^2. Figure 5(b) shows monthly variation of diffuse solar radiation (I_D). The maximum and minimum value of I_D during the study period are found 363.0 ± 87.9 W/m^2 in February and 107.7 ± 20.4 W/m^2 in July respectively due clear and cloudy day. Variation is large in March due to large value of standard deviation 122.6 W/m^2 and less in July due less value in standard deviation 20.4W/m^2.

Figure 5

Monthly Variation of Direct Solar Radiation and Diffuse Solar Radiation

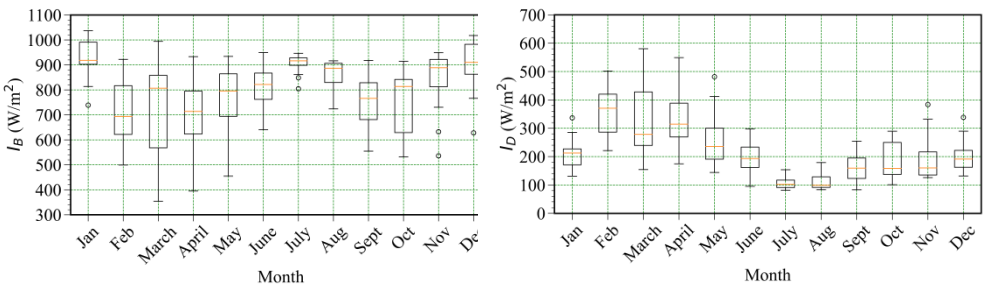

a) Monthly variation of direct solar radiation

b) Monthly variation of diffuse solar radiation

Figure 6 shows seasonal variation of direct solar radiation (I_B) and direct diffuse solar radiation (I_D). Figure 6(a) shows seasonal variation of direct solar radiation (I_B). The maximum and minimum value of I_B during the study period are found 856.2 ±93.2 W/m^2 in Winter and 738.5 ± 146.5 W/m^2 in spring respectively due to air pollution. Variation is large in spring due to large value of standard deviation 146.5 W/m^2 and less in summer due less value in standard deviation 66.8 W/m^2. Figure 6(b) shows seasonal variation of diffuse solar radiation (I_D). The maximum and minimum value of I_D during the study period are found 300.7 ± 99.6 W/m^2 in spring and 147.3 ± 43.1 W/m^2 in summer respectively. Variation is large in spring due to large value of standard deviation 99.6 W/m^2 and less in summer due less value in standard deviation 43.1 W/m^2.

Figure 6

Seasonal Variation of Direct Solar Radiation and Diffuse Solar Radiation

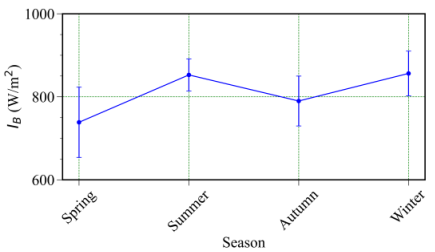

a) *Seasonal variation of direct solar radiation*

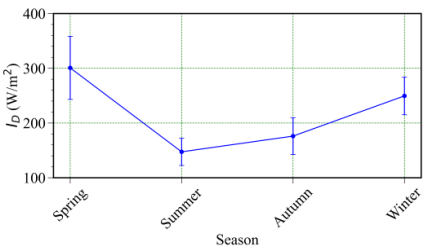

b) *Seasonal variation of diffuse solar radiation*

Seasonal variation of time series data are also analyzed by using Fourier series (Anton et al., 2011).

$$y_s = a_0 + a_1 \cos\left(\frac{2\pi}{365} n_d\right) + b_1 \sin\left(\frac{2\pi}{365} n_d\right) \quad (11)$$

Here a_0 is offset and $\sqrt{a_1^2 + b_1^2}$ gives amplitude of seasonal component. Offset and amplitude of seasonal component of direct solar radiation are found 807.2 W/m^2 and 45.4 W/m^2 respectively as shown in Figure 7(a). Offset and amplitude of seasonal component of diffuse solar radiation are found 218.6 W/m^2 and 97.3 W/m^2 respectively as shown in Figure 7(b). Due to large value of amplitude of seasonal component, diffuse solar radiation is seasonal dependent.

Figure 7

Fourier Analysis of Direct Solar Radiation and Diffuse Solar Radiation

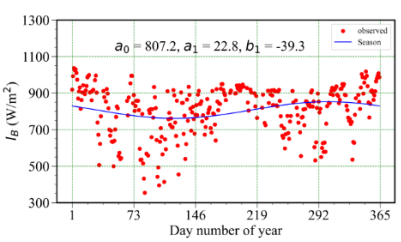

a) Fourier analysis of direct solar radiation

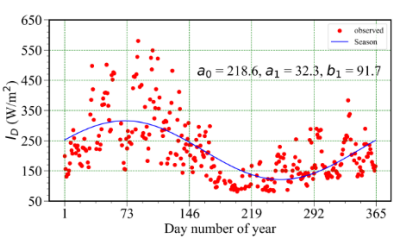

b) *Fourier analysis of diffuse solar radiation*

Figure 8(a) shows cross correlation between I_D and I_B with time lag in day. Correlation coefficient (r) is -0.83 at zero-day time lag. They are negatively corrected. When I_D increases, I_B decreases. They are fitted in straight line (y = mx + c) by best fit method as shown in figure 8(b). The straight line obtained with slope -0.6, y intercept is 735.8 and 69 % coefficient of determination (R^2).

Figure 8

Variation between Direct Solar Radiation and Diffuse Solar Radiation

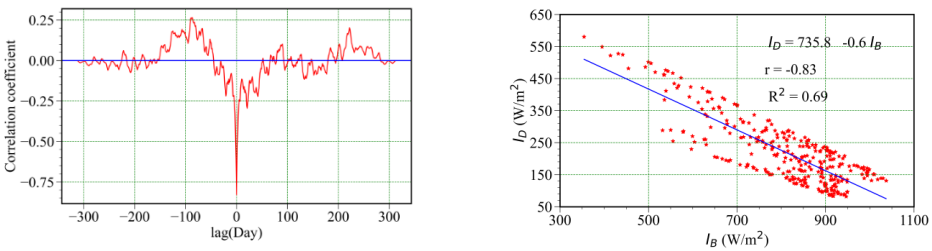

a) Cross correlation between I_B and I_D *b) Straight line*

4. Discussion

Datasets on solar radiation is of great importance to the detection of global dimming and brightening. Direct solar radiation and diffuse solar radiation estimation using easily available satellite data on basis of atmospheric transmittance. They are therefore important to propose solar energy potential of the location, the sustainable development of ecological environments and agriculture-based productivity. In study period of one year (2017) for Pokhara, the annual average of direct solar radiation and diffuse solar radiation are found 808.1± 133.7 W/m^2 and 220.8 ± 102.8 W/m^2 respectively at 12 PM NST. The Annual average of direct solar radiation is found 1106 ± 70 W/m^2 in Jomsom for a year 2012 (Shrestha et al., 2022). The annual average of diffuse solar radiation and direct solar radiation are found 216 ± 88 W/m^2 and 216±88 W/m^2 respectively on Bode, Bhaktapur on 2013 (Shrestha et al., 2022a). The annual average of diffuse solar radiation on Beijing and Lasa of China were to be 6.6 MJ/m^2/day (7.6 W/m^2) and 6.1 MJ/m^2/day (7.1 W/m^2) respectively from 1993 to 2015(Wang et al., 2019). Diffuse solar radiation is large on Pokhara than big city of China and India due to large amount of precipitation and air pollution.

Acknowledgments

The authors convey gratitude to faculty of Central Department of Physics, Department of Physics, Patan Multiple Campus, Institute of Science and Technology, Nepal Physical

Society and Association of Nepali Physicists in America for this opportunity. The authors like to acknowledge NASA for the data. We sincerely appreciate NAST for the PhD fellowship.

References

Adhikari, K. R., Bhattarai, B. K., & Gurung, S. (2013). Solar energy potential in nepal and global context. *Journal of the Institute of Engineering*, *9*(1), 96-106.

Angstrom, A. (1961). Techniques of determining the turbidity of the atmosphere. *Tellus*, *13*(2), 214-223.

Anton, M., Bortoli, D., Costa, M. J., Kulkarni, P. S., Domingues, A. F., Barriopedro, D., Serrano, A., & Silva, A. M. (2011). Temporal and spatial variabilities of total ozone column over Portugal. *Remote Sensing of Environmen*t, *115*(3), 855–863.

Bason, F. (2004). Diffuse solar irradiance and atmospheric turbidity. *In Euro Sun 2004* Conference Proceedings, Freiburg, Germany, pages 1–7.

Bintanja, R. (1996). The parameterization of shortwave and longwave radiative fluxes for use in zonally averaged climate models. *Journal of climate*, *9*(2), 439–454.

Bird, R. E., & Hulstrom, R. L. (1981). Simplified clear sky model for direct and diffuse insolation on horizontal surfaces. Technical report, *Solar Energy Research Inst., Golden, CO (USA)*.

CBS (2023). *National Population and Housing Census 2021*. Central Bureau of Statistics, National Planning Commission Secretariat, Government of Nepal.

Duffie, J. A., & Beckman, W. A. (2013). *Solar Engineering of Thermal Processes*. John Wiley & Sons.

Iqbal, M. (1983). *An Introduction to Solar Radiation*. New York: Academic Press.

Liou, K. N. (2002). *An introduction to Atmospheric Radiation* (2 ed.). Elsevier.

Lothian, G. F. (1963). Beer's Law and its Use in Analysis. A Review. *Analyst*, *88*(1050), 678–685.

Majupuria T. C. (1999). *Nepal nature's paradise: insight into diverse facets of topography, flora and ecology*. Gwalior: M. Devi.

MoF (2022). *Economic Survey 2021/022*. Ministry of Finance, Government of Nepal.

Poudyal, K. N. (2015). Estimation of global solar radiation using modified angstrom empirical formula on the basis of meterological parameters in himalaya region Pokhara, Nepal. *Journal of the Institute of Engineering*, *11*(1), 158–164.

Poudyal, K. N., Bhattarai, B. K., Sapkota, B., & Kjeldstad, B. (2012). Estimation of global solar radiation using clearness index and cloud transmittance factor at trans-himalayan region in Nepal. *Energy and power engineering*, *4*(6), 415.

Poudyal, K. N., Bhattarai, B. K., Sapkota, B., Kjeldstad, B., & Daponte, P. (2013). Estimation of the daily global solar radiation; Nepal experience. *Measurement*, *46*(6), 1807–1817.

Shrestha, P. M., Gupta, S. P., Joshi, U., Chapagain, N. P., Karki, I. B., & Poudyal, K. N. (2022). Estimation of direct solar radiation on high mountain region, Jomson, Nepal. *Patan Prospective Journal*, *2*(1), 221–231.

Shrestha, P. M., Gupta, S. P., Joshi, U., Chapagain, N. P., Karki, I. B., & Poudyal, K. N. (2022a). Estimation of direct and diffuse solar radiation on Bode, Bhaktapur. *Journal of Nepal Physical Society*, *8*(3), 20–25.

Wang, L., Chen, Y., Niu, Y., Salazar, G. A., & Gong, W. (2017). Analysis of atmospheric turbidity in clear skies at Wuhan, Central China. *Journal of Earth Science*, *28*(4), 729–738.

Wang, L., Lu, Y., Zou, L., Feng, L., Wei, J., Qin, W., & Niu, Z. (2019). Prediction of diffuse solar radiation based on multiple variables in china. *Renewable and Sustainable Energy Reviews*, *103*, 151–216.